POSTER REFERENCE: ICF100644PR

FATIGUE BEHAVIOR OF A MICRO-SIZED AUSTENITIC STAINLESS STEEL WITH FINE GRAINS

G. P. Zhang[1,2], K. Takashima[1], M. Shimojo[1] and Y. Higo[1]

[1] Precision and Intelligence Laboratory, Tokyo Institute of Technology
4259 Nagatsuta-cho, Midori-ku, Yokohama, 226-8503, Japan
[2] State Key Laboratory for Fatigue and Fracture of Materials, Institute of Metal Research
Chinese Academy of Sciences, 72 Wenhua Road, Shenyang 110015, P. R. China

ABSTRACT

A fine-grained (about 1-3 μm in diameter) austenitic stainless steel thin film was selected. Micro-cantilever beam type specimens were fabricated by focused ion beam (FIB) machining. The dynamic bending tests of the microbeams were carried out under constant load amplitude control. The cyclic strain hardening behavior was found in the material under two cyclic load amplitudes, ΔP=40 and 47 mN. At ΔP=47 mN, the significant intrusions formed on the sample surface due to the development of cyclic strain localization and provided the preferential site of microcrack initiation. Mode I fatigue crack propagation occurred in the fine-grained material by a transgranular mode. The dislocation microstructures of the fatigued micromaterial were investigated by TEM. The mechanism of fatigue damage in the material was discussed.

KEYWORDS

Micro-sized material, Austenitic stainless steel, Fine grain, Fatigue

INTRODUCTION

Great research interests on the measurement of Young's modulus, yield and fracture strength of all kinds of micromaterials were brought about due to miniaturization of materials in microelectromechanical systems (MEMS) devices [1-3]. However, as many microcomponents, such as micro radio frequency switches, etc. are constantly subjected to a cyclic load with a high frequency during the period of their service, fatigue properties of micro-sized materials should be a more important factor for a long-term reliability of microcomponents [4,5]. On the other hand, fine- or super fine- grained materials are widely used in MEMS devices in the form of thin films, which are deposited on Si substrates. Therefore, the study on mechanical properties, especially fatigue properties of such a fine-grained material provides not only a database of mechanical properties for the design of MEMS devices, but also an insight into the fundamental fatigue mechanism.

In this study, a micro-sized austenitic stainless steel with fine grains was selected. Fatigue properties of the fine-grained material were investigated by dynamic bending tests.

EXPERIMENTAL

The material used in this study was a commercial 304 stainless steel thin sheet with fine grains. The microstucture of the material observed by Focused Ion Beam (FIB) machining system exhibited that the grain size was about 1-3 μm in diameter, as shown in Fig. 1. The micro-cantilever beam type specimens were fabricated at the center of a 3 mm-diameter disk with 25μm thickness by FIB machining [6]. The dimensions and shape of the microbeam is shown in Fig. 2. The distance from the loading point to the fixed end of the microbeam was 50 μm.

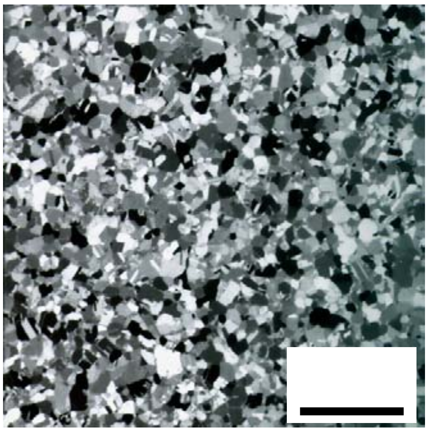

Figure 1: FIB observation of the grain size of the fine-grained austenitic stainless steel.

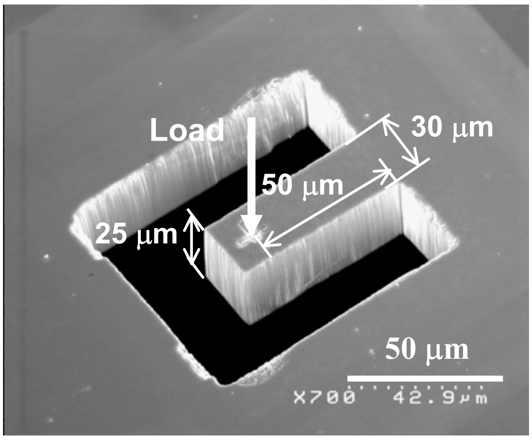

Figure 2: Dimensions and shape of the micro-cantilever beam type specimen fabricated by FIB machining.

Dynamic bending tests of the microbeams were carried out using a new type of fatigue testing machine for micro-sized specimens. This machine is of a displacement resolution of 5 nm and a load resolution of 10 μN [5]. The various waveforms for cyclic loading and frequencies up to 100 Hz can be applied using this machine. Before testing, the diamond tip was precisely located at the loading point by the repeated calibrations using the CCD camera, and then the micro-cantilever beam was dynamically bent under constant load amplitude control. The load ratio R ($R=P_{min}/P_{max}$) was 0.15 and the frequency was 10 Hz. All tests were stopped after about 4.5×10^5 cycles to examine fatigue damage on the specimen surfaces by scanning electron microscopy (SEM).

The deformed area of the microbeam was thinned by FIB machining to less than 0.1 μm to facilitate transmission electron microscopy (TEM) observations. The observation of dislocations was carried out with a Philips CM 200 type TEM at an accelerating voltage of 200 kV.

RESULTS AND DISCUSSION

1. Cyclic deformation behavior

The mean deflection δ_m (δ_m=(δ_{max}+δ_{min})/2) of the microbeam at the first cycle was set to be zero (δ_m=0), therefore, during cyclic loading if the microbeam moves downward gradually (the compliance of the beam increased), which is associated with the cyclic strain softening or cracking behavior of the material, δ_m will become negative. On the contrary, δ_m associated with the cyclic strain hardening behavior, will become positive, as schematically illustrated in Fig. 3(a). Figure 3(b) shows the variation of the mean deflection δ_m of the microbeam with cycles at both load amplitudes. It can be found that at ΔP=40 mN, the material initially experienced cyclic strain hardening and then cyclic hardening reached to a stable status gradually. The SEM examination on the top surface of the microbeam at the fixed end after 4.5×10^5 cycles exhibited that no microcracks initiated. When ΔP=47 mN, the material also exhibited the cyclic hardening behavior, but the maximum δ_m is higher than that at

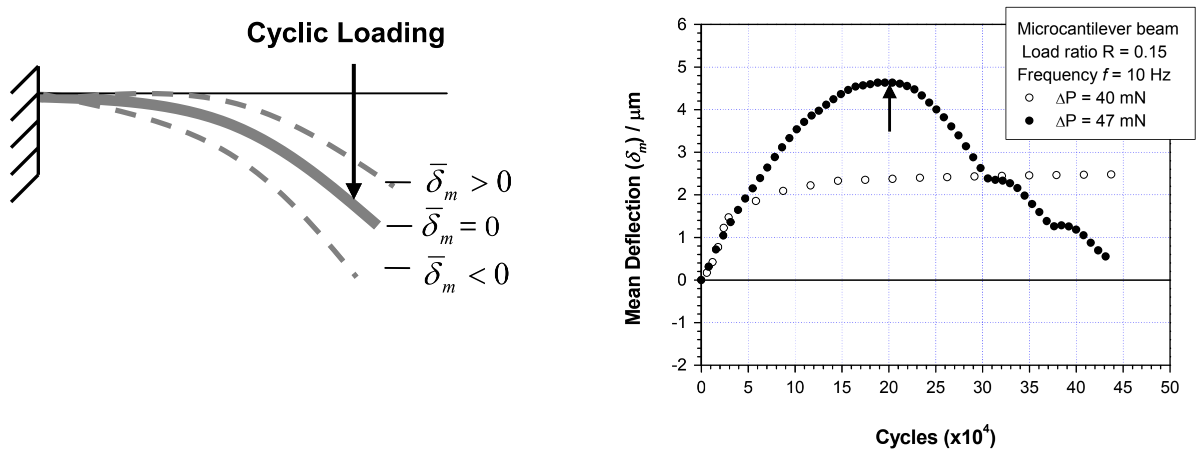

(a) **(b)**

Figure 3: (a) A schematic illustration of the variation of the mean deflection; (b) The variation of the mean deflection with cycles at both different load amplitudes.

ΔP=40 mN. With increasing cycles, δ_m decreased gradually after 2.0×10^5 cycles. The decrease of δ_m was identified to result from microcrack initiation and propagation in the material, as reported in the next section.

The stainless steels with grain sizes from several hundred microns to several tens of microns at a low strain amplitude usually exhibited primary cyclic hardening followed by cyclic softening [7]. At a certain strain amplitude, primary hardening was followed by cyclic softening, which was then followed by secondary hardening. However, in the present study, only cyclic hardening was found in the fine-grained material at two load amplitudes. Figure 4 shows a comparison of dislocation microstructures before and after cyclic bending. Before deformation, the material showed a rather low density of dislocation, i.e. almost free dislocations (see Fig. 4(a)). But a high density of dislocation and strong interaction of dislocations within the grain could be found after cyclic bending, as shown in Fig. 4(b). Therefore, dislocations rapidly multiplied and then interacted with each other by the to-and-fro motion under cyclic loading. This should be responsible for cyclic hardening observed here. Such an interaction of dislocations was also found in the same micromaterial subjected to static bending, which led to stage I hardening of stress-strain [6]. At ΔP=40 mN, the primary cyclic hardening and then gradually cyclic stability indicated that the cyclic plasticity caused by such a cyclic load amplitude was gradually exhausted by the interaction of dislocations within the fine grains. With increasing load amplitude, more hardening was naturally caused due to a larger cyclic plastic strain and the subsequent damage would be likely induced, as reported by follows.

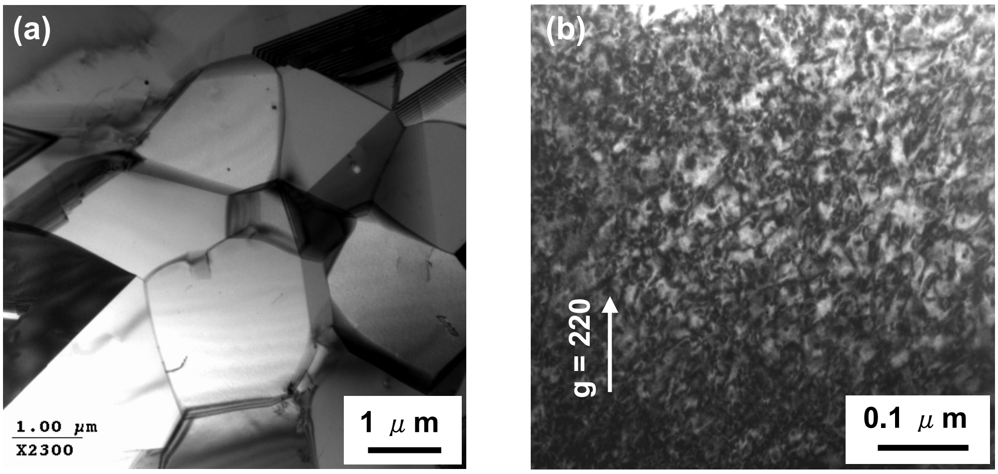

Figure 4: A comparison of dislocation microstructures in the fine-grained 304 stainless steel (a) before and (b) after cyclic bending.

2. *Fatigue damage*

The surface of the microbeam at ΔP=47 mN and about 4.5×10^5 cycles was examined by SEM. Figure 5 shows the whole view of the microbeam. A microcrack was found to initiate at the left corner of the fixed end and then gradually propagated toward the right side. The gradual decrease in δ_m at about 2.0×10^5 cycles was attributed to the microcrack initiation and subsequent propagation (see Fig. 3(b)). The crack propagation was perpendicular to the maximum tensile stress on the top surface and characterized by mode I cracking. A transgranular cracking was identified from the negative picture of the local area in Fig. 6(a), as shown in Fig.

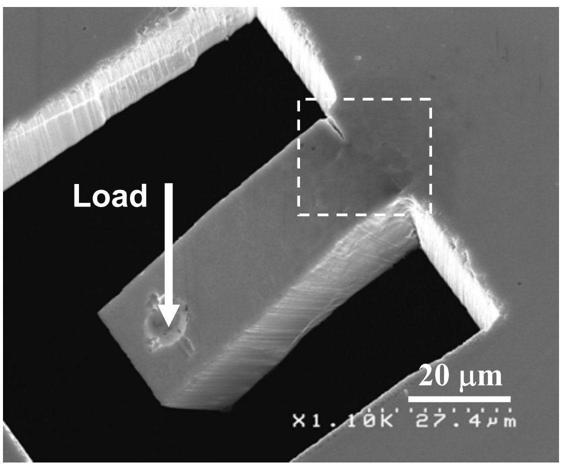

Figure 5: A whole view of the microbeam at ΔP=47 mN after about 4.5×10^5 cycles.

6(b). Especially, at the right corner of the fixed end circled by the white dot-line in Fig. 6(a), the slip traces within the grain became coarser and deeper preferentially. An enlargement of this area was presented in Fig. 7. Obviously, the strain localization developed in this area and resulted in some slip intrusions on the microbeam surface, as indicated by arrows. The depths of the intrusions **I** and **II** were about 0.56 and 0.24 μm measured by Scanning Laser Microscopy (SLM), respectively. The widths of the intrusions **I** and **II** were 0.38 and 0.22 μm, respectively.

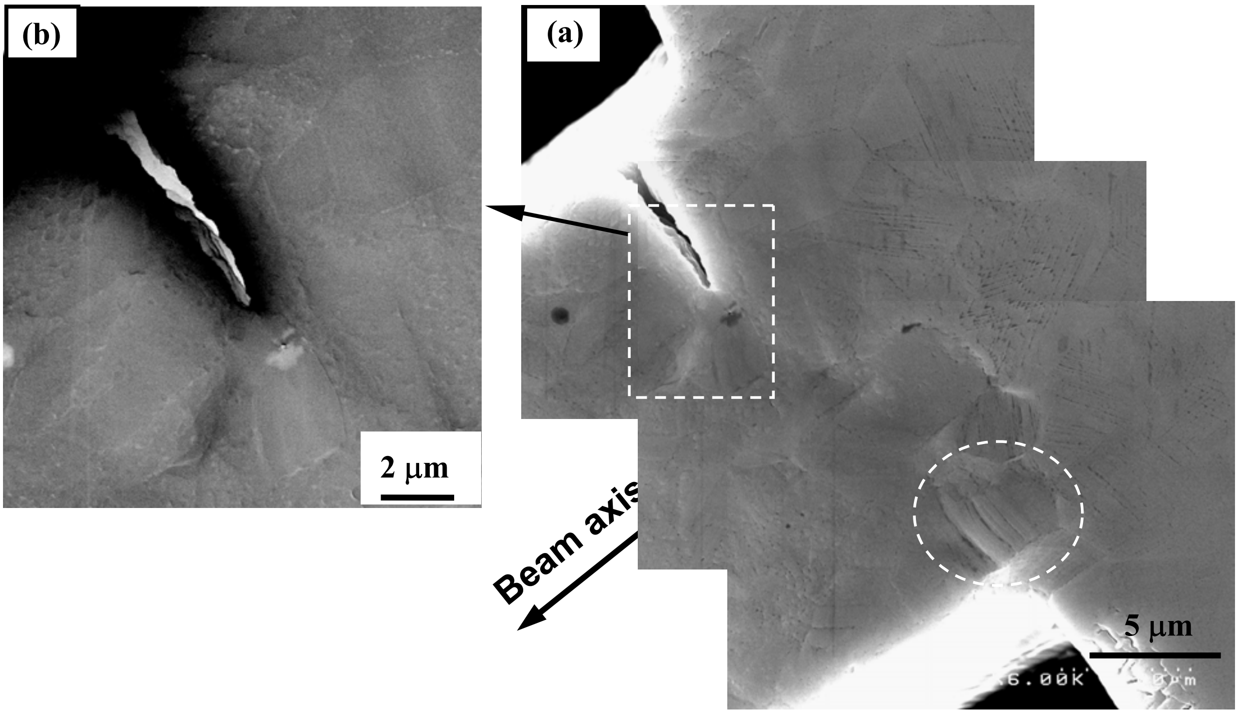

Figure 6: (a) A close observation of the surface of the microbeam cyclically bent at ΔP=47 mN after 4.5×10^5 cycles. (b) The negative picture shows a transgranular crack propagation.

The slip localization, which resulted in intrusions and extrusions on the specimen surface, are usually associated with the formation of PSB dislocation microstructures in single crystals, such as Cu, etc. under symmetrically cyclic plastic strain control [8]. However, at the present study, the slip intrusions on the micro-specimen surface were also found under asymmetrically cyclic load control, but no PSB microstructure

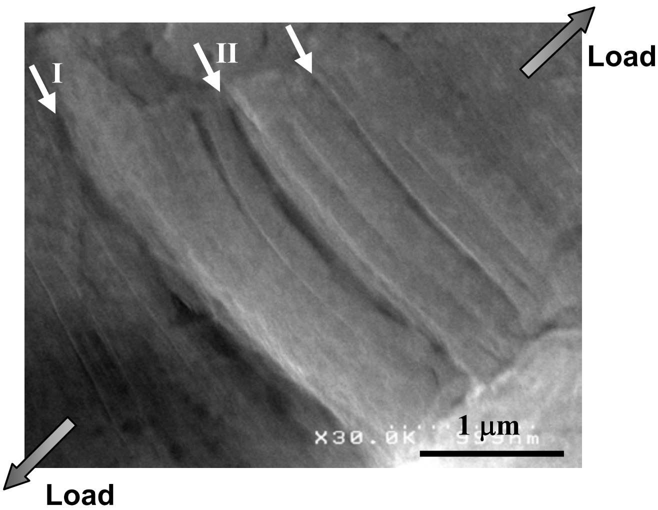

Figure 7: A high magnification of the strain localization within the grain developed at the fixed end of the microbeam circled by white dot-line in Figure 6(a).

was observed in the material, as shown in Fig. 4(b). Here, that a large number of dislocations slipped out of the specimen surface along preferentially oriented slip planes was suggested to be the reason for the formation of intrusions. While such coarse and deep slip traces were not observed in the same material subjected to static bending [6]. It is obvious that cyclic loading improved the strain localization. According to the measurement of the width and depth of the deepest intrusion **I**, it is reasonable to believe that such an intrusion with a depth of 0.56 μm and a root radius of 0.19 μm acted as a micro-notch. Therefore, the advancement of fatigue damage process in the micro-specimen with fine grains was as follows: under cyclic loading, some slip traces gradually developed to the coarse and deep slip traces, i.e. intrusions. These intrusions were of locally higher plastic strain at the intrusion root and more possibly became pre-sites of microcrack initiation. In general, cyclic strain localization still played an important role in microcrack initiation in the present micromaterial with fine grains and degraded the durability of the micromaterial.

CONCLUSTIONS

1. Cyclic strain hardening was found in the micro-sized austenitic stainless steel with fine grains. The strong interaction of dislocations was responsible for cyclic hardening.
2. The significant intrusions formed on the microbeam surface due to the development of cyclic strain localization. The microcracks were suggested to originate from the intrusions preferentially.
3. Mode I fatigue crack propagation occurred in the fine-grained material by a transgranular mode.

ACKNOWLEDGEMENTS

One of the authors (Zhang) would like to thank Japan Society for the Promotion of Science (JSPS) for the postdoctoral fellowship support (ID No. P99068).

REFERENCES

1. Ericson, F. and Schweitz, J. Å. (1990) *J. Appl. Phys*. 68, 5840.
2. Florando, J., Fujimoto, H., Ma, Q., Kraft, O., Schwaiger, R. and Nix, W. D. (1999) *MRS Symposium Proceedings*. *Materials Reliability in Microelectronics IX*. 353, 231.
3. Wilson, C. J., Ormeggi, A. and Narbutovskih, M. (1996) *J. Appl. Phys*. 79, 2386.
4. Schwaiger, R. and Kraft, O. (1999) *Scripta mater*. 41, 823.
5. Takashima, K., Higo, Y., Sugiura, S. and Shimojo, M. (2001) *Mater. Trans*. 42, 68.
6. Zhang, G. P., Takashima, K., Shimojo, M. and Higo, Y. (2000) *MRS Symposium Proceedings. Materials Science of Microelectromechanical Systems (MEMS) Devices III, edited by M. deBoer, M. Judy, H. Kahn and S. M. Spearing. 657, in press.*
7. Hennessy, D., Steckel, G. and Altstetter, C. (1976) *Metall. Trans*. 7A, 415.
8. Ma, B. T. and Laird, C. (1989) *Acta Metall*. 37, 325.